Chiral Triazole-substituted Iodonium Salts in Enantioselective Halogen Bond Catalysis

Mattis Damrath[a], Tarek Scheele[b], Daniel Duvinage[c], Tim Neudecker[bde], Boris J. Nachtsheim[a]*

[a]University of Bremen, Institute for Organic and Analytical Chemistry, 28359 Bremen, Germany
[b]University of Bremen, Institute for Physical and Theoretical Chemistry, 28359 Bremen, Germany
[c]University of Bremen, Institute for Inorganic Chemistry and Crystallography, 28359 Bremen, Germany
[d]University of Bremen, Bremen Center for Computational Materials Science, 28359 Bremen, Germany
[e]University of Bremen, MAPEX Center for Materials and Processes, 28359 Bremen, Germany

Prof. Dr. Boris J. Nachtsheim, nachtsheim@uni-bremen.de

Abstract

Herein, we present the synthesis of chiral triazole-based diaryliodonium salts and their application as monodentate asymmetric iodine(III) derivates in halogen bond (XB) catalyzed reactions. These potential Lewis acids were successfully benchmarked in the vinylogous Mannich reaction of cyanomethyl coumarin with isatin-derived ketimine to obtain the addition product in up to 99% yield and >99:1 *e.r.* Furthermore, these halogen bond catalysts allowed an efficient functionalization of ketimines with various alcohols toward *N,O*-acetals in up to 99% yield and 90:10 *e.r.* Additionally, we studied the origin of the enantioselectivity based on Density Functional Theory (DFT) and the catalyst crystal structure. These unveiled the first approach of asymmetric induction facilitated by using σ-hole stabilized chiral moieties in iodine(III)-based catalysts and exclusively predicated upon XB activation.

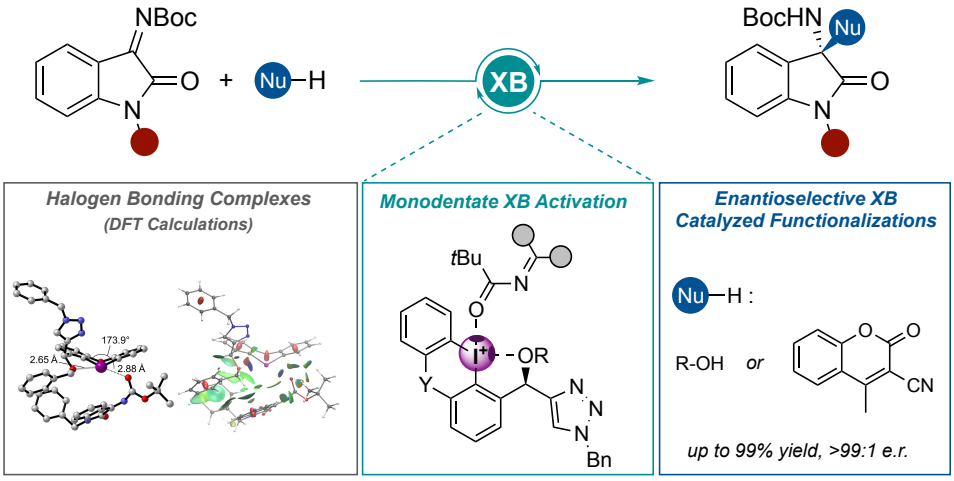

Keywords

organocatalysis • asymmetric catalysis • halogen bonding • hypervalent iodine • iodonium salts

Introduction

Over the last years, the utilization of halogen bonding[1] as a noncovalent interaction has been established in crystal engineering,[2] molecular recognition,[3] medicinal chemistry,[4] and organocatalysis.[5] Several mono- and multidentate iodine(I)-based XB donors, predominantly derived from dual iodo(benz)imidazolium or iodotriazolium motifs (Figure 1A), showed considerable strength as catalysts and can be referred to as halogen-based Lewis acids. For example, they efficiently catalyze halogen-abstraction reactions,[6] Nazarov cyclizations,[7] Diels-Alder reactions,[8] or Michael additions.[9]

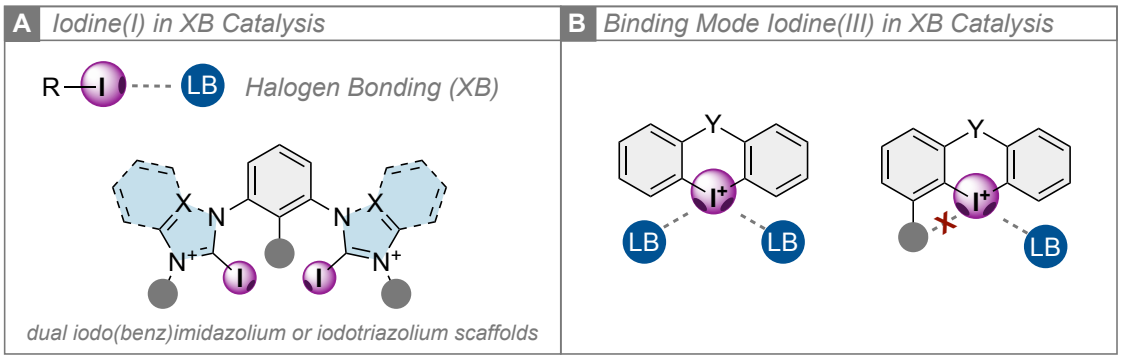

Figure 1. A) Iodine(I)-based activation mode in XB catalysis and commonly applied dual iodo(benz)imidazolium or iodotriazolium scaffolds. B) Binding mode of iodine(III)-based compounds in XB catalysis.

After extensive research and development of novel iodine (I) catalysts, the field was extended to iodine(III)-based XB donors by Han and coworkers in 2015.[10] They efficiently catalyzed a three-component Mannich reaction using electron-poor acyclic iodonium salts. Most of the iodine (III) XB donors so far are diaryliodonium salts with weakly coordinating anions, like BF_4^-, OTf^-, or $BArF^-$, to easily access the free cation for effective catalysis.[11] The synthesis of these compounds is simple: Oxidation of an iodoarene followed by acid-mediated ligand exchange with another aryl moiety yields the desired iodonium salts in general moderate to high yields depending on electronic and steric effects.[12] In 2017 and 2020, Legault and coworkers experimentally and computationally quantified the Lewis acidity of several diaryliodonium salts and compared them with conventional Lewis acids.[13] In 2018, the concept of Lewis acid-mediated catalysis was further examined by Huber and coworkers, verifying the XB-mediated

mechanism for diaryliodonium salts in halogen abstractions and Diels-Alder reactions.[14] Therein, they could show that *ortho*-substitution in cyclic diaryliodonium salts leads to blockage of the XB axis and results in deactivation of the catalyst (Figure 1B). In particular, cyclic iodonium salts have shown promising activity, and the more rigid structure compared to their acyclic counterparts can benefit their XB ability. In the following years, the research was focused on the development of stronger diaryliodonium salt-based XB catalysts. While Huber and coworkers established a thiophene-based bis-iodonium salt as a very potent bidentate XB donor,[15] Nachtsheim and coworkers were able to obtain similar or even higher activity in several benchmark reactions by introducing *N*-heterocyclic iod(az)olium salts and especially their *N*-methylated derivates.[16]

Most XB donors utilized so far were of an achiral nature,[5] with enantioselective adaptations of these catalytic processes being relatively underexplored. Several factors contribute to the increased complexity of achieving enantioinduction through XB in comparison to analogous hydrogen bond (HB) mediated enantioselective processes. Halogen bonding has a high directionality (with R-X···LB (Lewis base) angles approximating 180°), and this, combined with the elongated R-I and I···LB distances, results in a considerable spatial separation of the chiral backbone from the Lewis basic substrate. Furthermore, in contrast to hydrogen bonding, the design of chiral XB motifs demands a *de novo* approach, due to the absence of readily available templates. One feasible strategy to create a chiral environment proximal to the substrate entails integrating XB donor motifs into intricate interlocked systems.

First promising instances of enantioselective applications emerged by the groups of Tan[17] and Arai[18]. However, these examples involve XB as one interaction beside several other noncovalent interactions or by the introduction of Lewis/Brønsted-basic moieties to provide a more rigid chiral environment. In 2020, Huber and coworkers introduced novel bidentate chiral bis(imidazolium)-based iodine (I) halogen bond donors as the first example where the enantioinduction was solely reliant on XB (Scheme 1, A).[19] These bidentate catalysts were applied to the Mukaiyama aldol reaction with glyoxylates to yield the desired products in moderate enantioselectivities of up to 66.5:33.5 *e.r.*

Shortly afterward, Mancheño and coworkers reported a chiral tetrakis iodo-triazole system for enantioselective anion-binding catalysis.[20] While first obtaining comparable low enantioselectivities for a Reissert-type reaction, they just recently published a novel fine-tuning substrate-catalyst halogen-halogen interaction strategy to enable high enantiocontrol with up to 95:5 *e.r.* for the same reaction type.[21] In 2021, the first and so far only catalyst system for chiral halonium(III) based XB donors was reported by Yoshida and coworkers.[22] They used the

common chiral binaphthyl moiety with an additional HB donor to effectively catalyze the functionalization of isatin-derived ketimines in the vinylogous Mannich reaction with cyanomethyl coumarins or by simple addition of thiols in up to 98:2 *e.r.*[23]

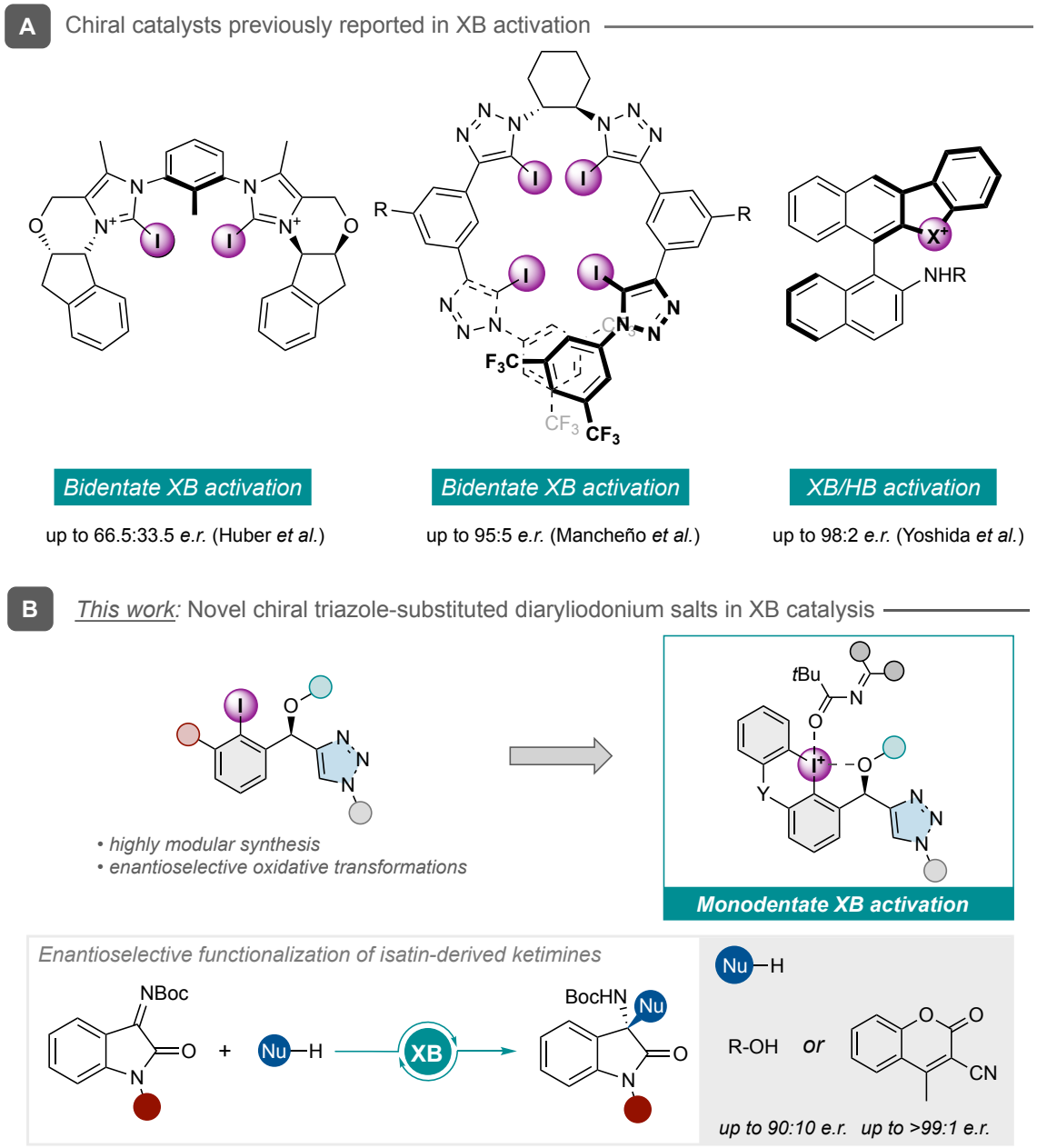

Scheme 1. A) Previously reported halogen bond (XB) catalysts for asymmetric transformations. B) This work: Synthesis of novel chiral triazole-based diaryliodonium salts and their application in XB catalysis.

In the present work, we want to present a novel catalyst system for underexplored enantioinduction by chiral iodine (III) based XB donors. Regarding our previously established and highly modular chiral triazole-based iodoarene scaffold for hypervalent iodine-mediated oxidative transformations,[24] we were interested if this chiral sidearm can also effectively catalyze enantiocontrolled XB reactions. Our initial idea was to use one σ-hole of the

diaryliodonium salt to interfere with the chiral sidearm (*O* or *N*-coordination could be possible) to build up a rigid structure with a defined chiral environment and the remaining σ-hole for the activation of the lewis basic substrate.

Results and Discussion

The synthesis of novel chiral triazole-based oxygen-bridged six-membered diaryliodonium salts **1** (Scheme 2) started from commercially available 3-hydroxybenzylalcohol (**3**), which was arylated in an Ullmann coupling with chlorobenzene followed by lithium-mediated iodination toward iodobenzyl alcohol **5** in 60% over 2 steps. For the five-membered diaryliodonium salts **2**, the synthesis started from readily available 3-bromo anthranilic acid (**4**). This compound was arylated in a Suzuki coupling, iodinated by Sandmeyer reaction, and followed by reduction to yield the corresponding benzyl alcohols **6** in high yields over 3 steps.

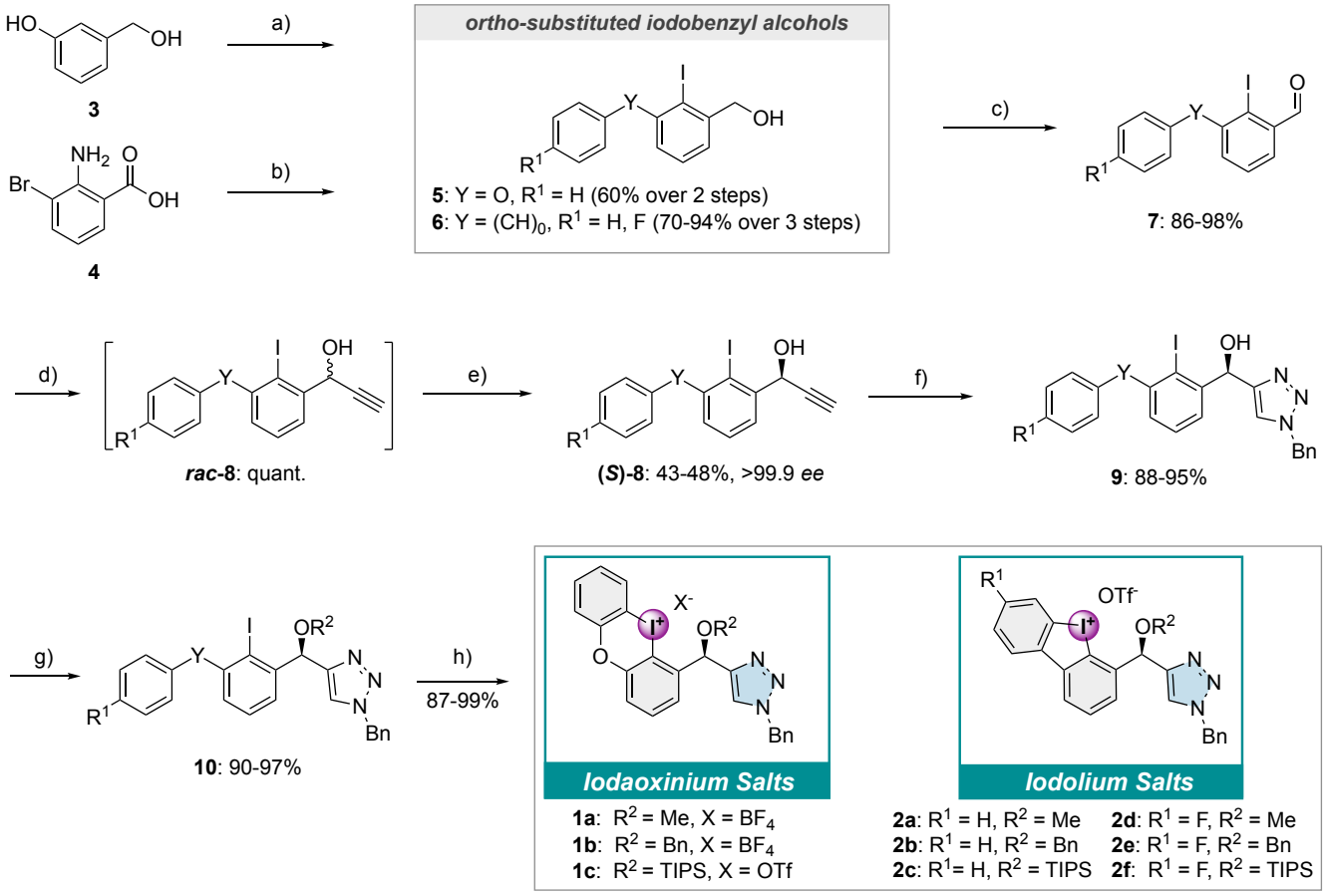

Scheme 2. Synthesis of novel chiral triazole-based diaryliodonium salts **1a-c and 2a-f**. Reaction conditions: a) i. PhCl, CuI, BPPO, K_3PO_4, DMSO ii. *n*BuLi, I_2, THF; b) i. R^1-$B(OH)_2$, $Pd(PPh_3)_4$, K_3PO_4, EtOH ii. $NaNO_2$, HCl, KI, H_2O iii. BH_3·DMS, THF; c) MnO_2, $CHCl_3$; d) EthynylMgBr, THF; e) CALB, isopropenyl acetate, Na_2CO_3, toluene; f) BnN_3, H_2O; g) R^2-X, THF/DMF or R^2-OTf, DCM; h) Selectfluor®, TfOH, MeCN or *m*CPBA, TfOH, DCM.

The alcohols **5** and **6** were oxidized quantitatively to the corresponding aldehydes **7** with MnO_2, followed by Grignard reaction and enzymatic resolution with CALB to the (*S*)-propargylic

alcohols **(*S*)-8** in good yields and with excellent enantioselectivities. Afterward **(*S*)-8** reacted with benzyl azide toward chiral triazole derivates **9** in high yields of up to 95%. These derivates were protected (Me, Bn, TIPS) nearly quantitatively toward compounds **10**. Subsequently, the oxygen-bridged derivates (except the TIPS-substituted) were oxidized and cyclized by our effective method for iodaoxinium salts[25] with Selectfluor® as oxidant and TfOH as acid to yield **1a-b** in up to 98%. The TIPS-substituted derivate **1c** and the five-membered counterparts **2a-f** were obtained through conventional synthetic methodologies for diaryliodonium salts with *m*CPBA as oxidant and TfOH as acid in high yields of up to 99%.

To explore our hypothesis on the activation of the substrate by one σ-hole and stabilization of the chiral moiety by the other σ-hole of the iodonium salt, the previously synthesized diaryliodonium salts **1** and **2** were initially benchmarked in the vinylogous Mannich reaction of cyanomethyl coumarin **12** with isatin-derived ketimine **13a** (Table 1).

Table 1. XB catalyst benchmark – Vinylogous Mannich reaction with cyanomethyl coumarin **12** and isatin-derived ketimine **13a** toward **14**.

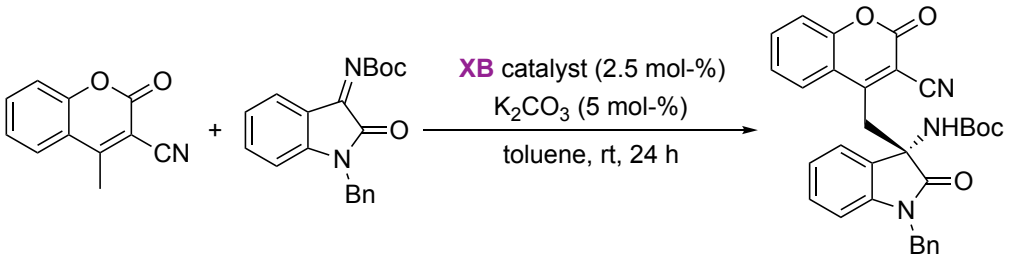

12 **13a** **14**

entry[a]	XB catalyst	yield / %	*e.r.*[b]
1	**1a**	74	>99:1
2	**1b**	82	>99:1
3	**1c**	69	>99:1
4	**2a**	80	18:82
5	**2b**	74	3:97
6	**2c**	65	90:10
7	**2d**	99	2.5:97.5
8	**2e**	52	3.5:96.5
9	**2f**	(60)[c]	55.5:44.5

[a] Reaction conditions: coumarin **12** (0.05 mmol, 1.0 eq.), isatin derivate **13a** (1.1 eq.), K_2CO_3 (5 mol-%), toluene (0.05 M).

[b] Determined via chiral HPLC analysis.

[c] Product/starting material mixture (1:1).

Surprisingly, almost all XB donors have shown excellent enantioselectivities at room temperature with moderate to excellent yields in this reaction. Particularly, with all oxygen-bridged diaryliodonium salts, the (*S*)-enantiomer of **14** was obtained in >99:1 *e.r.* (entry 1-3), while the benzyl-protected salt **1b** has shown the highest yield of 82% among them. Interestingly, the methyl and benzyl-protected five-membered analogs **2a** and **2b** revealed an almost complete reversal of the stereochemistry, yielding the (*R*)-enantiomer in up to 80% yield and up to 97:3 *e.r.* (entry 4 and 5) while the TIPS-protected salt gave the other enantiomer in a moderate yield of 65% with 90:10 *e.r.* (entry 6). By using the more electron-poor derivate **2d**, the yield could be increased to 99% with almost the same selectivity of 97.5:2.5 *e.r.* (entry 7), but the other analogs **2d** and **2f** have shown diminished yields and enantioselectivities (entry 8 and 9). While the yields and enantioselectivities were excellent, it was difficult to achieve insights regarding the activity and selectivity of these catalyst class because of the almost complete inversion of the enantioselectivity by just changing from the oxygen-bridged iodonium salts to the five-membered ones **2a-f**.

Since we knew that the isatin-derived ketimine **13a** could be excellently activated by our catalysts, we investigated in a less sterically and electronically simpler nucleophilic coupling reagent – benzyl alcohol (**15a**). Unfortunately, while conducting the first reactions with our XB catalysts we observed only low yields and enantiomeric ratios for the formation of the desired product **16a** beside decomposition products. Due to these circumstances, we performed a preoptimization of the reaction conditions (See ESI, Table S1). Under these optimized conditions, with K_2CO_3 as an additional base and toluene as the solvent, we have screened our triazole-based diaryliodonium salt XB catalysts at -10 °C (Table 2). It is worth mentioning that most of them, except the TIPS-protected iodonium salts, formed **16a** in nearly quantitative yields, while again the oxygen-bridged iodonium salts **1a-c** generally show higher enantioselectivities compared to their five-membered analogs **2a-f**.

Table 2 Catalyst screening of the XB catalyzed addition of benzyl alcohol (**15a**) to isatin-derived ketimine **13a** toward *N,O*-acetal **16a**.

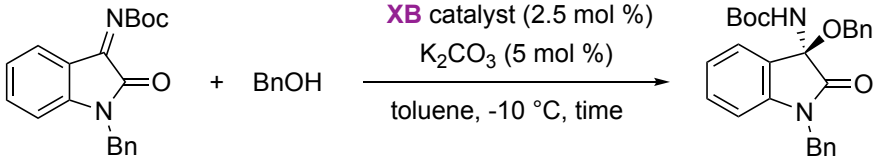

13a **15a** **16a**

entry[a]	XB catalyst	time / min	yield / %	*e.r.*[b]
1	**1a**	60	98	69:31
2	**1b**	60	99	76:24
3	**1c**	20	58	65:35
4	**2a**	60	97	64:36
5	**2b**	60	98	61:39
6	**2c**	20	43	59.5:40.5
7	**2d**	60	99	68:42
8	**2e**	60	97	61:39
9	**2f**	20	52	57.5:42.5

[a] Reaction conditions: isatin derivate **13a** (0.05 mmol, 1.0 eq.), BnOH (**15a**, 1.1 eq.), K_2CO_3 (5 mol%), toluene (0.05 M).

[b] Determined via chiral HPLC analysis.

In particular, the benzyl-protected salt **1b** has shown the most promising enantiocontrol with 76:24 *e.r.* Further optimizations with **1b** regarding base, catalyst loading, solvent, and temperature have not shown any improvement in this reaction (See ESI, Table S1-3).

With these conditions in hand, we further explored the substrate scope of this reaction (Scheme 3). By using the *ortho* methyl substituted benzylalcohol **15b** the *N,O*-acetal **16b** was obtained in 95% yield with an increased enantiomeric ratio of 90:10. When we used the 4-methylbenzyl alcohol (**15c**) instead, we observed the same enantioinduction like for the unsubstituted benzylalcohol of 76:24 *e.r.* This indicates that there might be steric or other noncovalent interactions in *ortho*-substituted substrates and ruled out their electronic properties. To further explore if more bulky groups can enhance the enantiocontrol we conducted the reaction with the ethyl, isopropyl, and *tert*-butyl-substituted benzylalcohols **15d-f**. While the ethyl-substituted product **16d** gave a slightly diminished enantiomeric ratio of 84:16, the more steric product **16e** was obtained only as the racemate, while the *t*Bu-substituted derivate **16f** could not be obtained under these reaction conditions. The 2,6-dimethyl-substituted benzyl alcohol **15g** yields the product **16g** in an almost similar enantiomeric ratio of 89:11 in comparison to the monomethyl-substituted derivate **16b** but in

just 64% yield due to prolonged reaction times. To further rule out the steric interactions for enantiocontrol we were able to generate the halogen-substituted products **16h** and **16i** in up to 98% yield, while the chloro-substituted derivate gave a superior enantiomeric ratio of 77:23 compared to the more sterically iodo-substituted counterpart with just 69:31 *e.r.*

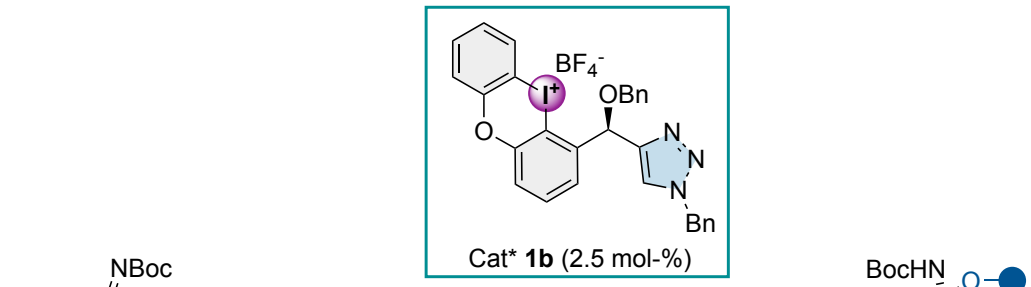

Alcohols

16a: Ar = Ph, >99%, 76:24 *e.r.*
16b: Ar = 2-Me-Ph, 95%, 90:10 *e.r.*
16c: Ar = 4-Me-Ph, 97%, 76:24 *e.r.*
16d: Ar = 2-Et-Ph, 94%, 84:16 *e.r.*
16e: Ar = 2-*i*Pr-Ph, 95%, *racemic*
16f: Ar = 2-*t*Bu-Ph, *no reaction*
16g: Ar = 2,6-Me-Ph, 64%, 89:11 *e.r.*
16h: Ar = 2-Cl-Ph, 98%, 77:23 *e.r.*
16i: Ar = 2-I-Ph, 94%, 69:31 *e.r.*
16j: Ar = 2-Ph-Ph, 99%, 85:15 *e.r.*
16k: Ar = 1-Naphtyl, 95%, 65:35 *e.r.*
16l: Ar = 2-OMe-Ph, 97%, 79:21 *e.r.*
16m: Ar = 2-NO_2-Ph, 84%, 66:34 *e.r.*
16n: Ar = 2-CF_3-Ph, 87%, 72:28 *e.r.*
16o: Ar = 2-Pyridyl, 91%, 59:41 *e.r.*
16p: Ar = 2-NHAc-Ph, 96%, 85:15 *e.r.*

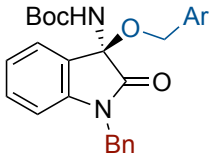

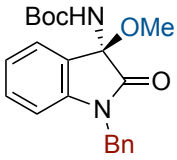

16q: 91%, 68:32 *e.r.*

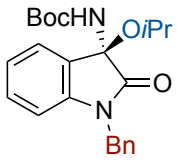

16r: 98%, 83:17 *e.r.*

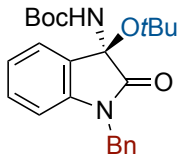

16s: *no reaction*

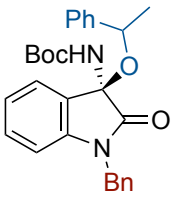

16t: 78%, 2:1 *d.r.*, 73:27 *e.r.*

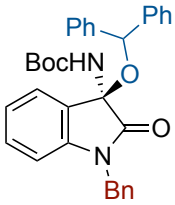

16u: 78%, 72:28 *e.r.*

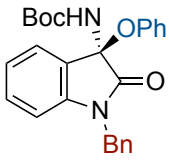

16v: *decomp.*

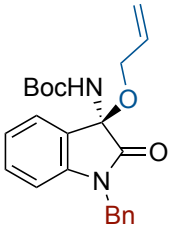

16w: 84%, 69:31 *e.r.*

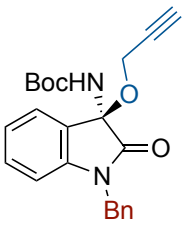

16x: 69%, *racemic*

Isatins

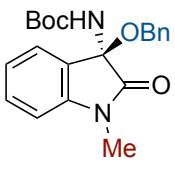

16y: 89%, 65:35 *e.r.*

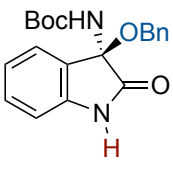

16z: 93%, *racemic*

Scheme 3. Substrate scope for the XB catalyzed addition of alcohols **15** to isatin-derived ketimines **13** toward *N,O*-acetals **16**. General reaction conditions: **13** (0.05 mmol, 1.0 eq.), **15** (1.1 eq), **1b** (2.5 mol-%), K_2CO_3 (5 mol-%), toluene (1 mL), -10 °C, 2 h.

To evaluate the effect of *ortho*-substituted benzylalcohols we conducted the reaction using phenyl-substituted benzylalcohol **15j** which yielded the acetal **16j** in an excellent yield of 99% and with 85:15 *e.r*. The naphthol derivate **16k** was obtained in 95% yield with just 65:35 *e.r.* More coordinating groups like OMe, NO_2, and CF_3 led to the products **16l-n** in high yields of up to 97% and with up to 79:21 *e.r.*, while the heterocyclic pyridyl benzylalcohol derivate **16o** was obtained in 95% yield with a low enantiomeric ratio of 65:35. By investigating the amide-substituted benzylalcohol **15p** as substrate, the acetal **16p** was yielded in 96% with a good enantiomeric ratio of 85:15. This might indicate a possible intermolecular hydrogen bonding of *ortho* substituents with the isatin-derived ketimine **13a** or the catalyst **1b**, which can increase the enantiocontrol by building a more rigid system for chirality transfer. The origin of the *ortho*-substituted substrate-dependent enantiocontrol is still under current investigation in our laboratory. We next expanded the substrate scope to alkyl alcohols. With methanol as the nucleophilic reagent, the product **16q** was obtained in 91% yield with moderate 68:32 *e.r*. Higher levels of enantioinduction could be observed by using isopropanol to yield *N,O*-acetal **16r** (83:17 *e.r.*) in comparable yields. The more steric *t*BuOH led not to product formation of **16s** under the investigated reaction conditions. Furthermore, using secondary benzyl alcohols **15t** and **15u** yielded the products **16t** and **16u** with almost the same enantioinduction (up to 77:23 *e.r.*) with a diastereomeric ratio of 2:1 for derivate **16t**. The reaction of isatin-derived ketimine **13a** with phenol led to the decomposition of the starting material, while allyl alcohol and propargyl alcohol yielded the desired products **16w** and **16x** in up to 84% yield but with low (69:31 *e.r.* for **16w**) or no enantioinduction. We further expanded the scope regarding isatin-derived ketimines **13**. The *N*-methyl-protected derivate **16x** was obtained in 89% yield with 65:35 *e.r*., while the unsubstituted ketimine **13c** led to racemic product formation in 93% yield. This indicates that *N*-protection is crucial for enantioinduction with our XB catalyst.

Furthermore, we were interested in the origin of enantioselectivity for our catalysts in the XB-mediated activation of isatin-derived ketimines. The X-ray structure was obtained for the methyl-protected iodaoxinium salt **1a** (Figure 1). This shows the typical T-shaped structure for iodine (III) compounds with one aryl moiety and the BF_4^- anion were located in apical positions. Interestingly, there is a clearly observable dative *O*-interaction derived from the methoxy substituent instead of an *N*-coordination from the triazole toward the hypervalent iodine center,

which was calculated to be more favorable in hypervalent iodine-mediated oxidative transformations.[26]

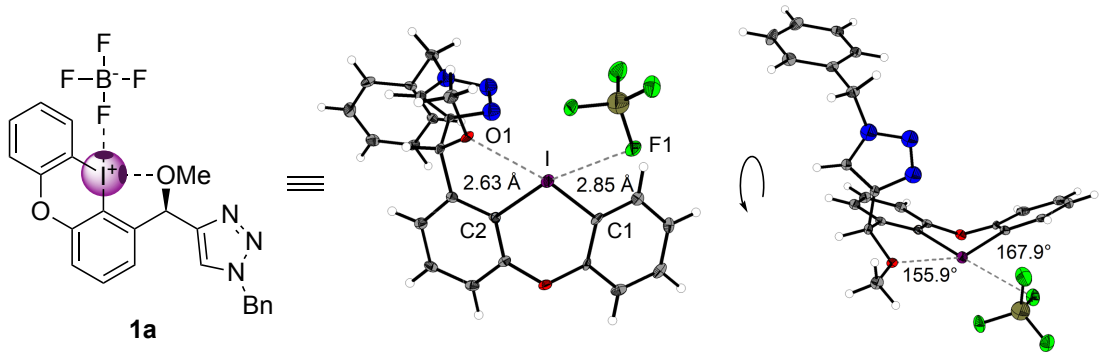

Figure 1. X-ray structural analysis of chiral XB catalyst **1a** (CCDC 2330036). Selected bond lengths (Å) and angles (°): I-O1: 2.63, I-F1: 2.85, C1-I-O1 155.9, C2-I-F1 167.9.

With this initial information in hand and to gain more insights into the interactions of the XB catalyst leading to enantioinduction, computational investigations based on density functional theory (DFT) were performed at the B3LYP-D3[27]/def2-TZVP[28] level of theory as implemented in ORCA 5.0.[29] The cation of the catalyst **1a** and isatin-derived ketimine **13a** were used to study possible activation complexes toward the formation of major and minor enantiomers (Figure 2, A). Among the different obtained activation complexes, **1a-COM** (major and minor) has shown the most probable state of activation in accordance with previously obtained experimental observations. Herein, we calculated a free Gibbs energy difference between the two possible complexes regarding the two enantiomers of 0.8 kcal mol^{-1}, which can already be a first indicator for the low enantiomeric induction through catalyst **1a**. However, the calculations show the XB interaction for the **1a-COM** (major) is stronger regarding the shorter distance (2.87 Å vs. 3.00 Å) and the NCI plot analysis (higher attractive interaction). It has also a more ordinary halogen bond interaction angle (167° vs 153°). In accordance with these results, we further calculated the halogen bonding complexes **1b-COM** (major and minor) of our best-performing catalyst **1b** (Figure 2, B). The free Gibbs energy difference of 3.4 kcal mol^{-1} between the two possible complexes is in good agreement with the experimental results showing a promising enantioinduction for the benzyl-substituted catalyst **1b**. The main factor for the higher enantioselectivity compared to the methyl-substituted derivate **1a** is due to a rising number of noncovalent interactions like CH-π or π-π interactions between the catalyst and the substrate. These interactions form a small pocket between the benzyl moiety of catalyst **1b** and the ketimine **13a**, indicative for the experimentally observed higher enantioinduction.

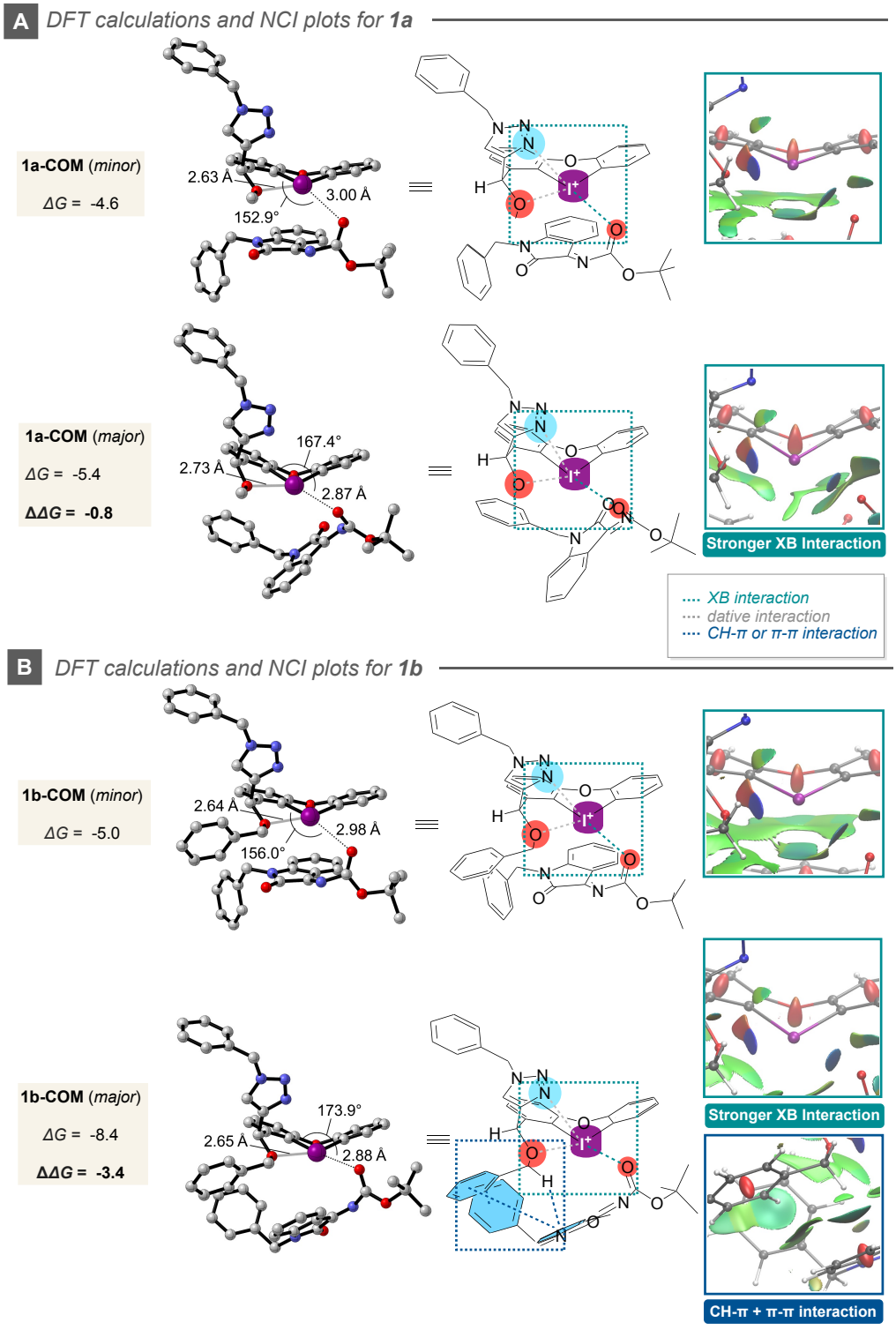

Figure 2. Visualization of structures and NCI plots of halogen bonding complexes **1a-COM** (A) and **1b-COM** (B), as obtained by DFT calculations (prepared with CYLview[30] and VMD[31]). Structure optimization and frequency analysis were performed at the B3LYP-D3/def2-TZVP level of theory using a continuum solvation model (C-PCM)[32] in toluene (ε = 2.4). The relative free energies (Δ*G* and ΔΔ*G* in kcal mol^{-1}) were calculated at 263 K. Color code for NCI plots: red = repulsion, green = van der Waals attraction/weak interaction (e.g. hydrogen bonding, halogen bonding), blue = strong interaction (e.g. hydrogen bonding, halogen bonding).

Summary

In conclusion, novel chiral triazole-based diaryliodonium salts were synthesized and introduced as effective XB donors in enantioselective halogen bond catalysis. In particular, the oxygen-bridged iodonium salts showed high performance and good selectivity in the investigated functionalizations of ketimines with up to 99% yield and >99:1 *e.r.* Further installation of more electron-deficient aryl moieties, especially *N*-heterocycles, in the iodonium system and fine-tuned chiral sidearms could allow more efficient transformations in the future. These additional variations and their implementation into bidentate structures are under current investigation in our laboratory.

Experimental Section

Detailed optimization studies, experimental procedures, analytical data (^{1}H-, ^{13}C- and ^{19}F-NMR-chemical shifts, IR-bands, melting points, optical rotations, HPLC chromatograms) including the corresponding NMR-spectra, X-ray data as well as the computational details can be found in the supporting information.

Acknowledgment

T.S. is grateful for financial support by the DFG (Deutsche Forschungsgemeinschaft, grant no. STA 1526/3-1, project no. 441071849).

References

(1) Cavallo, G.; Metrangolo, P.; Milani, R.; Pilati, T.; Priimagi, A.; Resnati, G.; Terraneo, G. The Halogen Bond. *Chem. Rev.* **2016**, *116* (4), 2478-2601. DOI: 10.1021/acs.chemrev.5b00484.
(2) (a) Metrangolo, P.; Meyer, F.; Pilati, T.; Resnati, G.; Terraneo, G. Halogen Bonding in Supramolecular Chemistry. *Angew. Chem. Int. Ed.* **2008**, *47* (33), 6114-6127. DOI: 10.1002/anie.200800128. (b) Gilday, L. C.; Robinson, S. W.; Barendt, T. A.; Langton, M. J.; Mullaney, B. R.; Beer, P. D. Halogen Bonding in Supramolecular Chemistry. *Chem. Rev.* **2015**, *115* (15), 7118-7195. DOI: 10.1021/cr500674c.

(3) (a) Taylor, M. S. Anion recognition based on halogen, chalcogen, pnictogen and tetrel bonding. *Coord. Chem. Rev.* **2020**, *413*, 213270. DOI: 10.1016/j.ccr.2020.213270. (b) Kampes, R.; Zechel, S.; Hager, M. D.; Schubert, U. S. Halogen bonding in polymer science: towards new smart materials. *Chem. Sci.* **2021**, *12* (27), 9275-9286. DOI: 10.1039/D1SC02608A.
(4) (a) Wilcken, R.; Zimmermann, M. O.; Lange, A.; Joerger, A. C.; Boeckler, F. M. Principles and Applications of Halogen Bonding in Medicinal Chemistry and Chemical Biology. *J. Med. Chem.* **2013**, *56* (4), 1363-1388. DOI: 10.1021/jm3012068. (b) Shinada, N. K.; de Brevern, A. G.; Schmidtke, P. Halogens in Protein–Ligand Binding Mechanism: A Structural Perspective. *J. Med. Chem.* **2019**, *62* (21), 9341-9356. DOI: 10.1021/acs.jmedchem.8b01453.
(5) (a) Bulfield, D.; Huber, S. M. Halogen Bonding in Organic Synthesis and Organocatalysis. *Chem. Eur. J.* **2016**, *22* (41), 14434-14450. DOI: 10.1002/chem.201601844. (b) Sutar, R. L.; Huber, S. M. Catalysis of Organic Reactions through Halogen Bonding. *ACS Catal.* **2019**, *9* (10), 9622-9639. DOI: 10.1021/acscatal.9b02894. (c) Breugst, M.; Koenig, J. J. σ-Hole Interactions in Catalysis. *Eur J Org Chem* **2020**, *2020* (34), 5473-5487. DOI: 10.1002/ejoc.202000660.
(6) Jungbauer, S. H.; Huber, S. M. Cationic Multidentate Halogen-Bond Donors in Halide Abstraction Organocatalysis: Catalyst Optimization by Preorganization. *J. Am. Chem. Soc.* **2015**, *137* (37), 12110-12120. DOI: 10.1021/jacs.5b07863.
(7) Dreger, A.; Wonner, P.; Engelage, E.; Walter, S. M.; Stoll, R.; Huber, S. M. A halogen-bonding-catalysed Nazarov cyclisation reaction. *Chem. Commun.* **2019**, *55* (57), 8262-8265. DOI: 10.1039/C9CC02816A.
(8) Jungbauer, S. H.; Walter, S. M.; Schindler, S.; Rout, L.; Kniep, F.; Huber, S. M. Activation of a carbonyl compound by halogen bonding. *Chem. Commun.* **2014**, *50* (47), 6281-6284. DOI: 10.1039/C4CC03124E.
(9) Gliese, J.-P.; Jungbauer, S. H.; Huber, S. M. A halogen-bonding-catalyzed Michael addition reaction. *Chem. Commun.* **2017**, *53* (88), 12052-12055. DOI: 10.1039/C7CC07175B.
(10) Zhang, Y.; Han, J.; Liu, Z.-J. Diaryliodonium salts as efficient Lewis acid catalysts for direct three component Mannich reactions. *RSC Adv.* **2015**, *5* (32), 25485-25488. DOI: 10.1039/C5RA00209E.
(11) Robidas, R.; Reinhard, D. L.; Legault, C. Y.; Huber, S. M. Iodine(III)-Based Halogen Bond Donors: Properties and Applications. *Chem. Rec.* **2021**, *21* (8), 1912-1927. DOI: 10.1002/tcr.202100119.
(12) (a) Merritt, E. A.; Olofsson, B. Diaryliodonium salts: a journey from obscurity to fame. *Angew. Chem. Int. Ed.* **2009**, *48* (48), 9052-9070. DOI: 10.1002/anie.200904689. (b) Chatterjee, N.; Goswami, A. Synthesis and Application of Cyclic Diaryliodonium Salts: A Platform for

Bifunctionalization in a Single Step. *Eur J Org Chem* **2017**, *2017* (21), 3023-3032. DOI: 10.1002/ejoc.201601651. (c) Peng, X.; Rahim, A.; Peng, W.; Jiang, F.; Gu, Z.; Wen, S. Recent Progress in Cyclic Aryliodonium Chemistry: Syntheses and Applications. *Chem. Rev.* **2023**, *123* (4), 1364-1416. DOI: 10.1021/acs.chemrev.2c00591.

(13) (a) Labattut, A.; Tremblay, P.-L.; Moutounet, O.; Legault, C. Y. Experimental and Theoretical Quantification of the Lewis Acidity of Iodine(III) Species. *J. Org. Chem.* **2017**, *82* (22), 11891-11896. DOI: 10.1021/acs.joc.7b01616. (b) Mayer, R. J.; Ofial, A. R.; Mayr, H.; Legault, C. Y. Lewis Acidity Scale of Diaryliodonium Ions toward Oxygen, Nitrogen, and Halogen Lewis Bases. *J. Am. Chem. Soc.* **2020**, *142* (11), 5221-5233. DOI: 10.1021/jacs.9b12998.

(14) Heinen, F.; Engelage, E.; Dreger, A.; Weiss, R.; Huber, S. M. Iodine(III) Derivatives as Halogen Bonding Organocatalysts. *Angew. Chem. Int. Ed.* **2018**, *57* (14), 3830-3833. DOI: 10.1002/anie.201713012.

(15) Heinen, F.; Reinhard, D. L.; Engelage, E.; Huber, S. M. A Bidentate Iodine(III)-Based Halogen-Bond Donor as a Powerful Organocatalyst**. *Angew. Chem. Int. Ed.* **2021**, *60* (10), 5069-5073. DOI: 10.1002/anie.202013172.

(16) (a) Boelke, A.; Kuczmera, T. J.; Caspers, L. D.; Lork, E.; Nachtsheim, B. J. Iodolopyrazolium Salts: Synthesis, Derivatizations, and Applications. *Org. Lett.* **2020**, *22* (18), 7261-7266. DOI: 10.1021/acs.orglett.0c02593. (b) Boelke, A.; Kuczmera, T. J.; Lork, E.; Nachtsheim, B. J. N-Heterocyclic Iod(az)olium Salts – Potent Halogen-Bond Donors in Organocatalysis. *Chem. Eur. J.* **2021**, *27* (52), 13128-13134. DOI: 10.1002/chem.202101961.

(17) Zong, L.; Ban, X.; Kee, C. W.; Tan, C.-H. Catalytic Enantioselective Alkylation of Sulfenate Anions to Chiral Heterocyclic Sulfoxides Using Halogenated Pentanidium Salts. *Angew. Chem. Int. Ed.* **2014**, *53* (44), 11849-11853. DOI: 10.1002/anie.201407512.

(18) (a) Arai, T.; Suzuki, T.; Inoue, T.; Kuwano, S. Chiral Bis(imidazolidine)iodobenzene (I-Bidine) Organocatalyst for Thiochromane Synthesis Using an Asymmetric Michael/Henry Reaction. *Synlett* **2017**, *28* (01), 122-127. DOI: 10.1055/s-0036-1588614. (b) Kuwano, S.; Suzuki, T.; Hosaka, Y.; Arai, T. A chiral organic base catalyst with halogen-bonding-donor functionality: asymmetric Mannich reactions of malononitrile with N-Boc aldimines and ketimines. *Chem. Commun.* **2018**, *54* (31), 3847-3850. DOI: 10.1039/C8CC00865E.

(19) Sutar, R. L.; Engelage, E.; Stoll, R.; Huber, S. M. Bidentate Chiral Bis(imidazolium)-Based Halogen-Bond Donors: Synthesis and Applications in Enantioselective Recognition and Catalysis. *Angew. Chem. Int. Ed.* **2020**, *59* (17), 6806-6810. DOI: 10.1002/anie.201915931.

(20) Ostler, F.; Piekarski, D. G.; Danelzik, T.; Taylor, M. S.; García Mancheño, O. Neutral Chiral Tetrakis-Iodo-Triazole Halogen-Bond Donor for Chiral Recognition and Enantioselective Catalysis. *Chem. Eur. J.* **2021**, *27* (7), 2315-2320. DOI: 10.1002/chem.202005016.

(21) Keuper, A. C.; Fengler, K.; Ostler, F.; Danelzik, T.; Piekarski, D. G.; García Mancheño, O. Fine-tuning Substrate--Catalyst Halogen--Halogen Interactions for Boosting Enantioselectivity in Halogen-Bonding Catalysis. *Angew. Chem. Int. Ed.* **2023**, *62*, e202304781. DOI: 10.1002/anie.202304781.

(22) Yoshida, Y.; Mino, T.; Sakamoto, M. Chiral Hypervalent Bromine(III) (Bromonium Salt): Hydrogen- and Halogen-Bonding Bifunctional Asymmetric Catalysis by Diaryl-λ3-bromanes. *ACS Catal.* **2021**, *11* (21), 13028-13033. DOI: 10.1021/acscatal.1c04070.

(23) Yoshida, Y.; Fujimura, T.; Mino, T.; Sakamoto, M. Chiral Binaphthyl-Based Iodonium Salt (Hypervalent Iodine(III)) as Hydrogen- and Halogen-Bonding Bifunctional Catalyst: Insight into Abnormal Counteranion Effect and Asymmetric Synthesis of N,S-Acetals. *Adv. Synth. Catal.* **2022**, *364* (6), 1091-1098. DOI: 10.1002/adsc.202101380.

(24) (a) Hempel, C.; Maichle-Mössmer, C.; Pericàs, M. A.; Nachtsheim, B. J. Modular Synthesis of Triazole-Based Chiral Iodoarenes for Enantioselective Spirocyclizations. *Adv. Synth. Catal.* **2017**, *359* (17), 2931-2941. DOI: 10.1002/adsc.201700246. (b) Abazid, A. H.; Nachtsheim, B. J. A Triazole-Substituted Aryl Iodide with Omnipotent Reactivity in Enantioselective Oxidations. *Angew. Chem. Int. Ed.* **2020**, *59* (4), 1479-1484. DOI: 10.1002/anie.201912023. (c) Abazid, A. H.; Clamor, N.; Nachtsheim, B. J. An Enantioconvergent Benzylic Hydroxylation Using a Chiral Aryl Iodide in a Dual Activation Mode. *ACS Catal.* **2020**, *10* (15), 8042-8048. DOI: 10.1021/acscatal.0c02321. (d) Abazid, A. H.; Hollwedel, T.-N.; Nachtsheim, B. J. Stereoselective Oxidative Cyclization of N-Allyl Benzamides to Oxaz(ol)ines. *Org. Lett.* **2021**, *23* (13), 5076-5080. DOI: 10.1021/acs.orglett.1c01607. (e) Abazid, A. H.; Nachtsheim, B. J. Application of chiral triazole-substituted iodoarenes in the enantioselective construction of spirooxazolines. *Chem. Commun.* **2021**, *57* (70), 8822-8825. DOI: 10.1039/D1CC03246A.

(25) Damrath, M.; Caspers, L. D.; Duvinage, D.; Nachtsheim, B. J. One-Pot Synthesis of Heteroatom-Bridged Cyclic Diaryliodonium Salts. *Org. Lett.* **2022**, *24* (13), 2562-2566. DOI: 10.1021/acs.orglett.2c00691.

(26) Golub, T. P.; Abazid, A. H.; Nachtsheim, B. J.; Merten, C. Structure Elucidation of In Situ Generated Chiral Hypervalent Iodine Complexes via Vibrational Circular Dichroism (VCD). *Angew. Chem. Int. Ed.* **2022**, *61* (50), e202204624. DOI: 10.1002/anie.202204624.

(27) (a) Becke, A. D. Density-functional thermochemistry. III. The role of exact exchange. *J. Phys. Chem.* **1993**, *98* (7), 5648-5652. DOI: 10.1063/1.464913. (b) Becke, A. D. Density-functional

exchange-energy approximation with correct asymptotic behavior. *Phys. Rev. A* **1988**, *38* (6), 3098-3100. DOI: 10.1103/PhysRevA.38.3098. (c) Lee, C.; Yang, W.; Parr, R. G. Development of the Colle-Salvetti correlation-energy formula into a functional of the electron density. *Phys. Rev. B* **1988**, *37* (2), 785-789. DOI: 10.1103/PhysRevB.37.785. (d) Stephens, P. J.; Devlin, F. J.; Chabalowski, C. F.; Frisch, M. J. Ab Initio Calculation of Vibrational Absorption and Circular Dichroism Spectra Using Density Functional Force Fields. *J. Phys. Chem.* **1994**, *98* (45), 11623-11627. DOI: 10.1021/j100096a001. (e) Grimme, S.; Antony, J.; Ehrlich, S.; Krieg, H. A consistent and accurate ab initio parametrization of density functional dispersion correction (DFT-D) for the 94 elements H-Pu. *J. Chem. Phys.* **2010**, *132* (15). DOI: 10.1063/1.3382344. (f) Grimme, S.; Ehrlich, S.; Goerigk, L. Effect of the damping function in dispersion corrected density functional theory. *J. Comp. Chem.* **2011**, *32* (7), 1456-1465. DOI: 10.1002/jcc.21759.

(28) (a) Weigend, F.; Ahlrichs, R. Balanced basis sets of split valence, triple zeta valence and quadruple zeta valence quality for H to Rn: Design and assessment of accuracy. *Phys. Chem. Chem. Phys.* **2005**, *7* (18), 3297-3305. DOI: 10.1039/B508541A. (b) Weigend, F. Accurate Coulomb-fitting basis sets for H to Rn. *Phys. Chem. Chem. Phys.* **2006**, *8* (9), 1057-1065. DOI: 10.1039/B515623H. (c) Peterson, K. A.; Figgen, D.; Goll, E.; Stoll, H.; Dolg, M. Systematically convergent basis sets with relativistic pseudopotentials. II. Small-core pseudopotentials and correlation consistent basis sets for the post-d group 16–18 elements. *J. Phys. Chem.* **2003**, *119* (21), 11113-11123. DOI: 10.1063/1.1622924.

(29) (a) Neese, F. The ORCA program system. *Wiley Interdiscip. Rev. Comput. Mol. Sci.* **2012**, *2* (1), 73-78. DOI: 10.1002/wcms.81. (b) Neese, F. Software update: the ORCA program system, version 4.0. *Wiley Interdiscip. Rev. Comput. Mol. Sci.* **2018**, *8* (1), e1327. DOI: 10.1002/wcms.1327. (c) Neese, F. Software update: The ORCA program system—Version 5.0. *Wiley Interdiscip. Rev. Comput. Mol. Sci.* **2022**, *12* (5), e1606. DOI: 10.1002/wcms.1606.

(30) Legault, C. Y. CYLview, 1.0b. http://www.cylview.org: Université de Sherbrooke, 2009.

(31) Humphrey, W.; Dalke, A.; Schulten, K. VMD - Visual Molecular Dynamics. *J. Molec. Graph.* **1996**, *14*, 33-38. DOI: 10.1016/0263-7855(96)00018-5.

(32) Cossi, M.; Rega, N.; Scalmani, G.; Barone, V. Energies, structures, and electronic properties of molecules in solution with the C-PCM solvation model. *J. Comp. Chem.* **2003**, *24* (6), 669-681. DOI: 10.1002/jcc.10189.